Constitutive equation with internal damping for materials under cyclic and dynamic loadings using a fully coupled thermal-structural finite element analysis

Ladislav Écsi and Pavel Élesztős
Institute of Applied Mechanics and Mechatronics,
Faculty of Mechanical Engineering,
Slovak University of Technology in Bratislava, Námestie slobody 17
812 31 Bratislava, Slovakia
ladislav.ecsi@stuba.sk, pavel.elesztos@stuba.sk

ABSTRACT

In this paper a universal constitutive equation with internal damping for materials under cyclic and dynamic loading is presented using fully coupled thermal-structural finite element analysis. The equation adapts the idea of a spring dashpot system connected in parallel for continuum utilizing appropriate deformation measures, which are independent of rigid body motion, thus enabling more precise numerical simulation of real material. In this work, mathematical formulation of the problem is presented and demonstrated in numerical examples using a solid bar in cyclic tension and a cross-shaped specimen in biaxial tension. Elastic and plastic loading cases with and without heat generation rate per unit volume were studied, where the heat generation rate was defined as 80% of the dissipated energy per unit time. Although the calculation results are in good agreement with the only experiment we could find in technical literature, more detailed tests are needed to draw final conclusions.

1. INTRODUCTION

Dissipative processes that take place in material outside thermal equilibrium play an important role in deformable body behaviour. One such dissipative process is an internal damping which can essentially affect the construction behaviour. Contemporary theories don't pay too much attention to the problem and the induced thermo-mechanical processes are not sufficiently understood. In the presented paper, a universal constitutive equation with internal damping is presented. The model adapts the idea of a spring-dashpot system connected in parallel for continuum utilizing appropriate deformation measures, which are independent of rigid body motion, thus enabling more precise numerical simulation.

2. THEORY BACKGROUND

In the presented work we assume that the deformations of a solid body, idealized as non-polar continuum [1], [2], are infinitesimal. In the energy conservation equation derivation we keep strictly to basic principles of thermodynamics [3], [4] and work with known and experimentally verified physical quantities. We neither strive for completeness nor try to include any dissipative process into the analysis [5]–[8], which may take place in the material, but its mathematical formulation has not been yet clarified or verified experimentally.

2.1. THE GOVERNING EQUATIONS OF THE BODY

The local form of conservation of energy of a closed thermodynamic system; a solid deformable body is given in the following form [9]:

$$\mathbf{v}\bullet(\rho\dot{\mathbf{v}}-\mathbf{b}-\nabla\bullet\boldsymbol{\sigma})+\dot{e}-(\boldsymbol{\sigma}:\mathbf{d}-\nabla\bullet\mathbf{q}+r)=0. \tag{1}$$

Here $\boldsymbol{\sigma}$, $\boldsymbol{d}$, $\boldsymbol{q}$, $\boldsymbol{b}$, $\boldsymbol{v}$, e, r, ρ respectively denote the Cauchy stress tensor, the strain rate tensor, the heat flux vector, the body force vector, the velocity vector, the internal energy per unit volume, the heat generation rate per unit volume and the material density at a material point of the body. From the physical point of view, the first part of Eqn (1) represents the power of mechanical forces, which is also known as the local form of the conservation of mechanical energy

$$\mathbf{v}\bullet(\rho\dot{\mathbf{v}}-\nabla\bullet\boldsymbol{\sigma}-\mathbf{b})=\rho\dot{\mathbf{v}}\bullet\mathbf{v}+\boldsymbol{\sigma}:\mathbf{d}-\nabla\bullet(\boldsymbol{\sigma}\bullet\mathbf{v})-\mathbf{b}\bullet\mathbf{v}=0, \tag{2}$$

and the second part is a heat equation, which represents the local form of the conservation of heat energy. In contemporary literature [5], [6], [8], [10] the heat equation is often incorrectly denoted as the local form of the conservation of energy and its final form, suitable for calculation, is derived from assumed energy functionals, in which local state axioms and thermodynamic constraints coming from the second law of thermodynamics [5], [6] are applied. Such a heat equation will work properly if and only if all assumptions in its derivation are correct. Instead of using the aforementioned procedure in our study a simpler heat equation is employed

$$\dot{e}-(\boldsymbol{\sigma}:\mathbf{d}-\nabla\bullet\mathbf{q}+r)=\rho c\dot{T}+\nabla\bullet\mathbf{q}-r=0, \tag{3}$$

in which c and T respectively stand for the specific heat capacity and the temperature. Moreover, we may say that the equation is complete and applicable for both, elastic and plastic loading, if we reinterpret the meaning of its last term in the sense that any heat, generated during the deformation of the body, can be viewed as a heat generation rate per unit volume. After substituting Eqns (2) and (3) into Eqn (1) the final form of the conservation of energy will be recovered, which in harmony with Eqn (3) will imply that $\dot{e}=\rho c\dot{T}+\boldsymbol{\sigma}:\mathbf{d}$. The same formula could be found more easily by simply applying the definition of the first principle of thermodynamics, i.e. balancing the energy fluxes, over the body using known physical quantities only.

From the conventional solution point of view of a system of partial differential equation (PDE) [11], any of Eqns (1) or (3) supplemented with the Euler-Cauchy equation of motion

$$\rho\dot{\mathbf{v}}-\nabla\bullet\boldsymbol{\sigma}-\mathbf{b}=\mathbf{0},\qquad \boldsymbol{\sigma}=\boldsymbol{\sigma}^{\mathrm{T}}, \tag{4}$$

form an equivalent system of PDE, the solution of which is identical and as a result Eqn (1) can be replaced with Eqn (3). The same, however, does not apply in the case of the weak solution [11], [12], as the energy functionals created from any of the aforementioned system will result in different solution at their extremes, which we will discuss later.

In order to solve the governing equations of the body, Eqns (3) and (4) are supplemented with constitutive equations and boundary conditions (BC). We are particularly interested in the case where the boundary conditions take the form

$$\text{BC: } -\mathbf{q}\bullet\mathbf{n}=q_n=h\left(T_{BULK}-T_S\right), \tag{5}$$

$$\boldsymbol{\sigma}\bullet\mathbf{n}=\mathbf{t}. \tag{6}$$

Here $\mathbf{n}$, $\mathbf{t}$, h, T_s, T_{BULK} respectively denote the outward surface normal vector, the surface traction vector, the heat transfer coefficient, the surface temperature and the bulk temperature. If heat convection takes place, i.e. Eqn (5) applies, the heat equation cannot be solved alone using the conventional solution, regardless of the definition of the heat generation rate per unit volume. In this case, the temperature field and the deformation field of the body are coupled via Eqn (6), into which additional constraints have to be introduced, to get a solution.

Since Eqns (5) and (6) are not solved directly during the weak solution, only their left-hand sides are replaced with their right-hand sides in the energy functional appropriate term integration [11], [12], in the weak solution Eqn (1) cannot be replaced with Eqn (3), as in the functional the conservation of mechanical energy ensures the two-way coupling represented by the second BC. The governing equations of the body then take the following variational forms [13], [14]

$$\int_\Omega \rho\dot{\mathbf{v}}\bullet\delta\mathbf{v}dv+\int_\Omega \boldsymbol{\sigma}:\delta\mathbf{d}dv=\int_\Omega \mathbf{b}\bullet\delta\mathbf{v}dv+\int_{\partial\Omega}\mathbf{t}\bullet\delta\mathbf{v}ds+\sum_{i=1}^{NNode}\mathbf{f}_i\bullet\delta\mathbf{v}_i, \tag{7}$$

$$\begin{aligned}&\int_\Omega \delta T\rho\dot{\mathbf{v}}\bullet\mathbf{v}dv+\int_\Omega \delta T(\boldsymbol{\sigma}:\mathbf{d})dv+\int_\Omega(\nabla\delta T)\bullet(\boldsymbol{\sigma}\bullet\mathbf{v})dv+\int_\Omega \delta T\rho c\dot{T}dv-\int_\Omega(\nabla\delta T)\bullet\mathbf{q}dv=\\&=\int_\Omega \delta T\mathbf{b}\bullet\mathbf{v}dv+\int_{\partial\Omega}\delta T\mathbf{t}\bullet\mathbf{v}ds+\int_{\partial\Omega}\delta Tq_n ds+\int_\Omega \delta Trdv+\sum_{i=1}^{NNode}\delta T_i\mathbf{f}_i\bullet\mathbf{v}_i+\sum_{i=1}^{NNode}\delta T_iQ_i,\end{aligned} \tag{8}$$

where
$$\mathbf{q}=-\mathbf{K}\bullet(\nabla T). \tag{9}$$

Here $\mathbf{K}$, $\mathbf{f}_i$,$\mathbf{v}_i$,Q_i denote the conductivity tensor, the nodal force vector, the nodal velocity vector and the nodal heat flux at $i = 1,2,...,NNode$ nodes.

2.2. CONSTITUTIVE EQUATION WITH INTERNAL DAMPING

Considering the analogy between continuum and a spring dashpot system connected in parallel, where the spring force/damping force depends on the relative displacement/relative velocity of the spring ends, the Cauchy stress tensor of a material with internal damping can be expressed in the following incremental form [15]

$${}^{n+1}\boldsymbol{\sigma}={}^{n+1}\boldsymbol{\sigma}^{el}+{}^{n+1}\boldsymbol{\sigma}^{damp}, \tag{10}$$

where

$${}^{n+1}\boldsymbol{\sigma}^{el}=\Delta\boldsymbol{\sigma}^{el}+{}^{n}\boldsymbol{\sigma}^{el}, \tag{11}$$

$$\Delta\boldsymbol{\sigma}^{el}=\Delta t\mathbb{C}:\left({}^{n+\frac{1}{2}}\mathbf{d}-{}^{n+\frac{1}{2}}\mathbf{d}^{th}\right)\text{- in elastic loading / unloading,} \tag{12}$$

$$\Delta\boldsymbol{\sigma}^{el}=\Delta t\,\mathbb{C}:\left({}^{n+\frac{1}{2}}\mathbf{d}-{}^{n+\frac{1}{2}}\mathbf{d}^{th}-{}^{n+\frac{1}{2}}\mathbf{d}^{pl}\right)\text{- in plastic loading,} \tag{13}$$

$${}^{n+1}\boldsymbol{\sigma}^{damp}=\mathbb{C}_{damp}:{}^{n+1}\mathbf{d}. \tag{14}$$

In Eqns (10)–(14) the left superscripts $n, n+\frac{1}{2}, n+1$ denote the physical quantity value at discrete times, corresponding to the previous, mid and current configuration of the body. We assume that the material is isotropic and the strain rate tensor has the additive decomposition $\mathbf{d} = \mathbf{d}^{el} + \mathbf{d}^{pl} + \mathbf{d}^{th}$ into an elastic part $\mathbf{d}^{el}$, a plastic part $\mathbf{d}^{pl}$ and a thermal part $\mathbf{d}^{th} = \alpha \dot{T} \mathbf{I}$. Here α is the coefficient of thermal expansion, $\dot{T}$ the temperature change per unit time and $\mathbf{I}$ is a unit second-order tensors. Eqns (10)–(14) are supplemented with the following constitutive and evolution equations

$$f = \sigma_{eq} - \sigma_y - R \le 0, \tag{15}$$

$$\sigma_{eq} = \sqrt{\frac{3}{2}\left(\boldsymbol{\Sigma} - \mathbf{X}\right) : \left(\boldsymbol{\Sigma} - \mathbf{X}\right)}, \tag{16}$$

$$R = Q\left(1 - e^{(-b\varepsilon^{pl})}\right), \tag{17}$$

$$\dot{\mathbf{X}} = \mathbb{C}_{cycl} : \mathbf{d}^{pl} - \gamma(\varepsilon^{pl})\mathbf{X}\dot{\varepsilon}^{pl}; \quad tr(\mathbf{X}) = 0, \tag{18}$$

$$\gamma(\varepsilon^{pl}) = \gamma_\infty - (\gamma_\infty - \gamma_0)e^{(-\omega\varepsilon^{pl})}. \tag{19}$$

Eqn (11) defines the elastic part of the Cauchy stress tensor, where the elastic stress increment $\Delta\boldsymbol{\sigma}^{el}$ is given either with Eqn (12) in elastic loading/unloading or with Eqn (13) in plastic loading. Here $\mathbb{C}$, Δt denote the fourth-order elastic material tensor and the time step size. Eqn (14) defines the damping part of the Cauchy stress tensor. Eqns (15)–(19) formulate the yield surface and the evolution equations of the extended NoIHKH material model [16], [17] using associative plasticity. The NoIH rule [18] for isotropic hardening and the NoKH rule [18] for kinematic hardening are given with Eqns (17)–(18). Here $\boldsymbol{\Sigma}$, $\mathbf{X}$, ε^{pl}, $\dot{\varepsilon}^{pl}$ respectively are the deviatoric component of the stress tensor, the back stress tensor, the accumulated plastic strain and the accumulated plastic strain rate. The remaining symbols denote constant material parameters. The fourth-order cyclic material tensor $\mathbb{C}_{cycl}$ and the damping tensor $\mathbb{C}_{damp}$ are formally constructed in the same way as the elastic material tensor using two independent variables v_{cycl}, E_{cycl} and v_{damp}, E_{damp}, which ensures isotropy

$$\mathbb{C}_i = 2G_i\mathbb{I} + \lambda_i(\mathbf{1}\otimes\mathbf{1}), G_i = \frac{E_i}{2(1+\nu_i)}, \lambda_i = \frac{\nu_i E_i}{(1+\nu_i)(1-2\nu_i)}, \tag{20}$$

for $i = cycl$, $damp$, where $\mathbb{I}$ is a unit fourth-order tensors.

2.3. DISSIPATION INDUCED HEATING

During deformation certain amount of the supplied mechanical energy dissipates into heat. To determine the exact portion of the dissipated energy that changes into heat represents a difficult experimental task [19], [20]. In this paper, we assume that this figure is around 80% and then we define the heat generation rate per unit volume as follows

$$r = 0.8\boldsymbol{\sigma} : \mathbf{d}^{pl} + 0.8\boldsymbol{\sigma}^{damp} : \mathbf{d}. \tag{21}$$

Here the first term on the right-hand side denotes the plastic heating and the second term stands for the internal damping induced heating.

3. NUMERICAL EXAMPLES

3.1. EXAMPLE NO. 1 – CYCLIC TENSION OF A STEEL BAR

In the first numerical experiment a solid bar, size 1m × 1m × 3m, was studied applying cyclic tension. One end of the bar was fixed and the second end underwent a prescribed axial deformation determined by a sine function and amplitude 2.5/3.5 mm corresponding to elastic/plastic loading case, while it was guided in the remaining two directions. The velocity and the acceleration of the bar end were defined as the first and second derivatives of the prescribed axial deformation. In the numerical experiment one loading cycle was realized using 15 degree angular increments in each time step. Cases with and without internal damping and with and without heat generation rate per unit volume were studied, using 0.04 *Hz,* 4.16 *Hz* and 41.66 *Hz* loading frequency corresponding to 1.0*s*, 0.01*s* and 0.001*s* time step values. The analyses were run as transient-dynamic ones considering heat convection through all surfaces and zero bulk temperature. The bar was initially at rest with zero initial temperature. The initial velocity of the body changed linearly in axial direction from zero at the fixed end to the maximum at the moving end of the bar to prevent initial oscillations in the run-up stage. Then we can say that in the numerical simulation a stabilized cycle was modelled without the initial transition stage that would vanish after few cycles due to internal damping. In the numerical experiment all material parameters were constant and, moreover, some of them have to be considered informative as their values were not determined experimentally. Table 1 shows the used material properties.

Figure 1 shows the temperature distribution in one longitudinal section of the bar at maximum tension corresponding to the plastic loading case using 41.66 Hz loading frequency, and the dissipated energy induced heating defined with Eqn (21). Figures 2-3 show the axial deformation versus axial stress curves at selected nodes, at the bar moving end N30 and in its middle part at node N149 (See Figure 1 for the location of the nodes). As can be seen in figure 2, there is no energy dissipation in elastic loading without damping, the system is conservative and the axial deflection versus axial stress curve is linear. Applying internal damping hysteresis loops were created and the material curve is no longer linear. Figures 2 and 3 imply that the area of the hysteresis loop is proportional to the deformation rate, i.e. the higher the deformation rate the greater the loop area as well as the amount of the dissipated energy. Also, in limiting state, as the deformation rate approaches zero, the effect of the internal damping vanishes.

Figures 4-5 depict the temperature time history at nodes N30, N149 in term of dimensionless time, defined as the ratio of the current time and the analysis end time. In the figures 25 multiply of the accumulated plastic strain time history is also depicted at node 149. There are great differences in temperature time history curves, depending on if elastic/plastic deformation takes place. In elastic loading the temperature change frequency is twice of the mechanical loading frequency. Figure 4 implies that there is a significant temperature rise at node N30, when the bar undergoes plastic deformation, although no plastic deformation has taken place at node N30.

3.2. EXAMPLE NO. 2 – CROSS SHAPED SPECIMEN IN BIAXIAL TENSION

In the second numerical experiment a cross shaped specimen under biaxial tension was studied. Figure 6 depicts the specimen geometry, the body of which contains 60 mm long and 0.2 mm wide axial cuts, to homogenize the stress field at its centre. In the numerical study only 1/8 of the specimen was modelled employing 3 planes of symmetry, while the fillets and the axial cuts were neglected. The body was loaded gradually applying constant axial velocity v = 0.15 mm/s and zero acceleration at its four ends. The maximum prescribed

Table 1 Material properties of the bar

E[Pa]	E_{cycl}[Pa]	E_{damp}[Pa·s]	$\nu = \nu_{cycl} = \nu_{damp}$[-]	σ_y [Pa]
$2.1 \cdot 10^{11}$	$2.1 \cdot 10^{5}$	0.0 / $2.1 \cdot 10^{8}$	0.3	$200.0 \cdot 10^{6}$
Q[Pa]	b[-]	γ_∞ [-]	γ_0 [-]	ω [-]
$50.0 \cdot 10^{6}$	3.0	20.0	10.0	10.0
ρ[kg/m^3]	c[J/kg·K]	$k_{xx} = k_{yy} = k_{zz}$[W/m·K]	$\alpha_x = \alpha_y = \alpha_z$[K^{-1}]	h [W/m^2·K]
7800.00	500.00	45.00	0.0000126	50.00

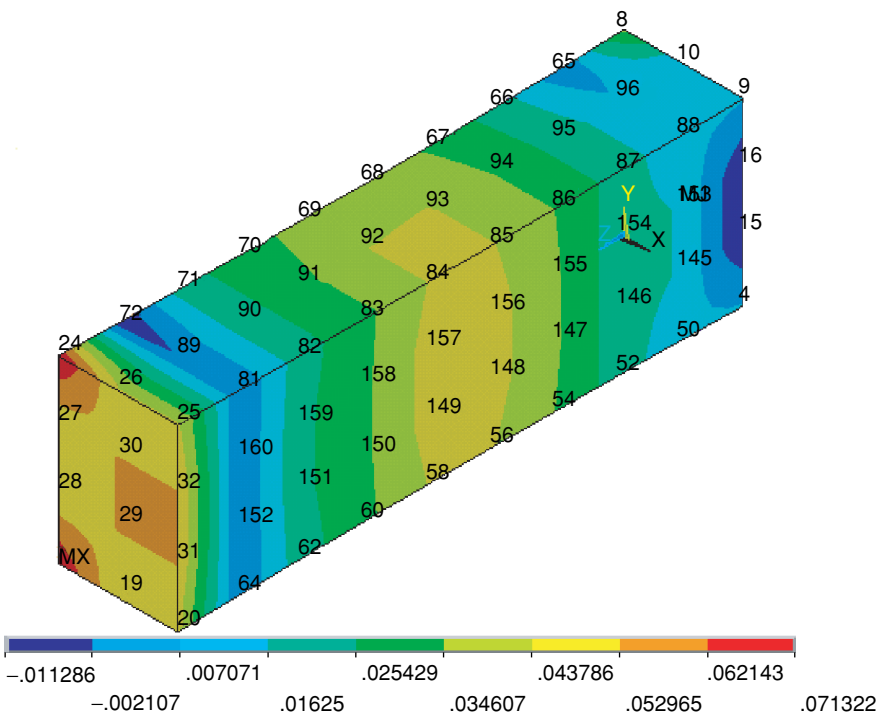

Figure 1 Temperature distribution in one longitudinal section of the bar at maximum tension.

deformation of the specimen end, 0.6mm, was achieved in 4 seconds using 26 time steps. Heat convection through all surfaces was considered, applying zero bulk/environmental temperature. The body was initially at rest with zero initial temperature. The analyses were run as transient-dynamic ones applying 0.154s time step size. In the numerical study constant material properties of pure aluminum and the Von-Mises material model were used, where the later is a special case of the extended NoIHKH material model without kinematic hardening. Table 2 outlines the material properties of the specimen.

Figure 7 shows the temperature time history at the centre of the cross-shaped specimen. In the first analysis only plastic heating was considered as a result of neglecting the material damping, while in the second analysis 80% of all dissipated mechanical energy contributed

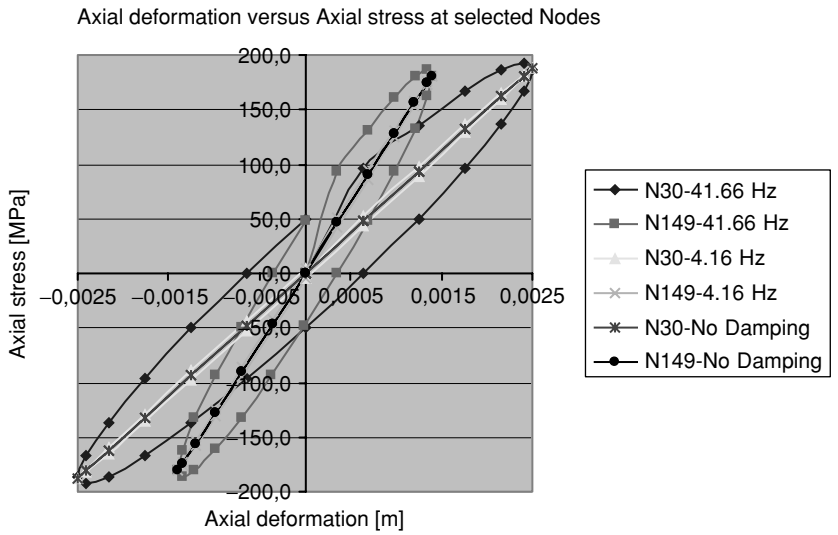

Figure 2 Hysteresis loops at selected nodes coming from the elastic loading case.

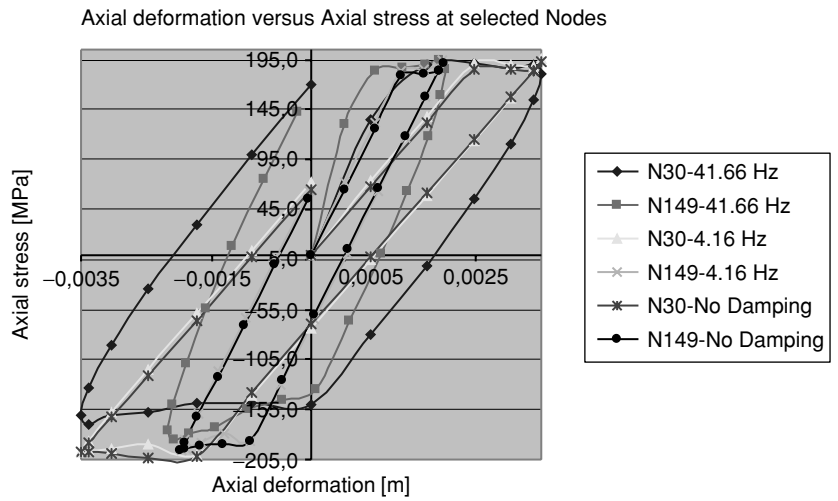

Figure 3 Hysteresis loops at selected nodes coming from the plastic loading case.

to the heating. Similar temperature profile can be seen in an only available experiment carried out on an AlMgSu1 cross-shaped specimen [21]. Figure 7 implies that the internal damping induced heating is probably overestimated, while the plastic heating seems to be more realistic. In spite of the fact that we don't know many details of the experiment, such as the material properties of the specimen or its exact dimensions, applied loading rates etc., the achieved results are very positive.

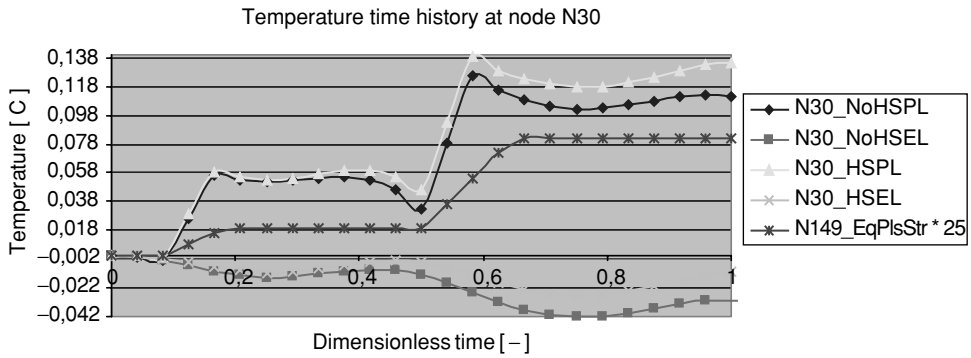

NoHSPL — No heat generation rate per unit volume and plastic loading case
NoHSEL — No heat generation rate per unit volume and elastic loading case
HSPL — Heat generation rate per unit volume and plastic loading case
HSEL — Heat generation rate per unit volume and elastic loading case
EqPlsStr * 25 — 25 times the actual accumulated plastic strain value

Figure 4 Temperature time history at node N30 using 44.61 Hz loading frequency.

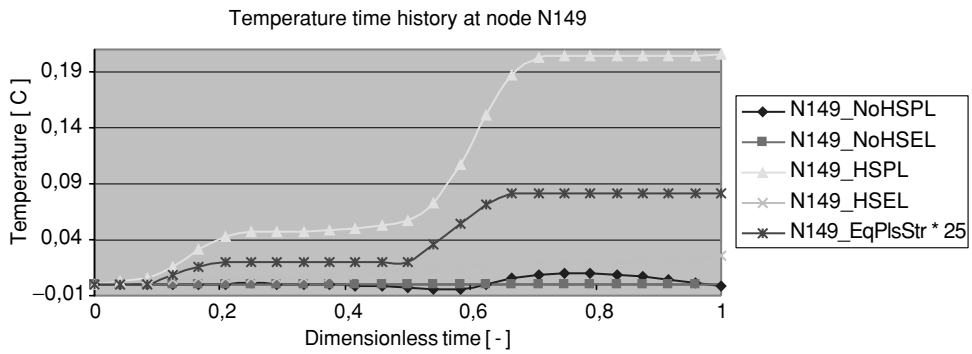

NoHSPL — No heat generation rate per unit volume and plastic loading case
NoHSEL — No heat generation rate per unit volume and elastic loading case
HSPL — Heat generation rate per unit volume and plastic loading case
HSEL — Heat generation rate per unit volume and elastic loading case
EqPlsStr * 25 — 25 times the actual accumulated plastic strain value

Figure 5 Temperature time history at node N149 using 44.61 Hz loading frequency.

4. CONCLUSION

In this paper a universal constitutive equation with internal damping was presented using fully coupled thermal structural finite element analysis. A solid bar in cyclic tension and a cross-shaped specimen in biaxial tension were studied. The analyses were capable to reproduce the temperature profile at the centre of a cross shaped specimen in harmony with the only available experiment. The achieved results are very positive; however they cannot be considered to be conclusive, as many details of the experiment have not been known. More detailed tests will be needed to draw final conclusions.

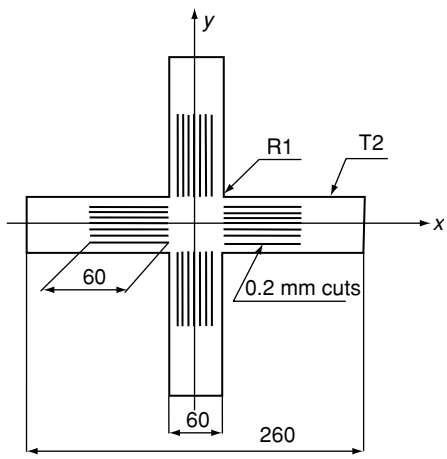

Figure 6 Specimen geometry.

Table 2 Material properties of the cross shaped specimen

E[Pa]	E_{cycl}[Pa]	E_{damp}[Pa·s]	$\nu = \nu_{cycl} = \nu_{damp}$[-]	σ_y [Pa]
$68.0 \cdot 10^9$	0.0	$0.0/68.0 \cdot 10^7$	0.36	$150.0 \cdot 10^6$
Q [Pa]	b [-]	γ_∞ [-]	γ_0 [-]	ω [-]
$50.0 \cdot 10^6$	3.0	0.0	0.0	10.0
ρ[kg/m^3]	c[J/kg·K]	$k_{xx} = k_{yy} = k_{zz}$[W/m·K]	$\alpha_x = \alpha_y = \alpha_z = \alpha$ [K^{-1}]	h [W/m^2·K]
2699.00	900.00	210.00	0.000024	50.00

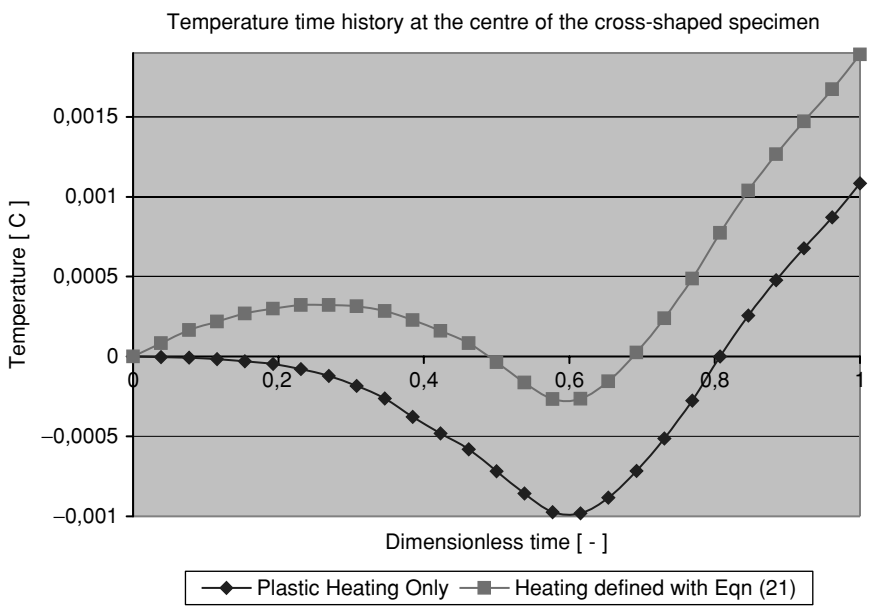

Figure 7 Temperature time history at the centre of the specimen

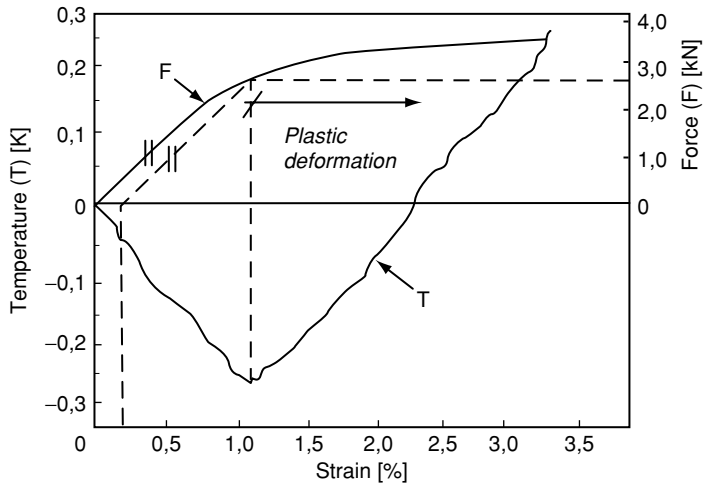

Figure 8 Temperature time history in terms of strain at the centre of a cross-shaped specimen after Franke H [21]

ACKNOWLEGEMENT

Funding using the VEGA grant No. 1/4103/07 resources is greatly appreciated. The paper was presented during the ACE-X 2008 conference.

REFERENCES

[1] HOLZAPFEL, G. A., Nonlinear solid mechanics, A continuum approach for engineering, John Wiley & Sons LTD., Chichester, 2001.

[2] BONET, J., WOOD, R. D., Nonlinear continuum mechanics for finite element analysis, Cambridge University Press, Cambridge, 1997.

[3] BIRD, R. B., STEWART, W. E., LIGHTFOOT, E. N., Transport phenomena, 2nd. Ed., John Wiley & Sons INC, NY, 2003.

[4] STEGER, H. G., SIEGHART, J., GLAUNINGER, E.: Műszaki mechanika 3, Termodinamika, szilárdságtan, rezgéstan, Műszaki Könyvkiadó, Budapest, 1995.

[5] MAUGIN, G.A., The thermomechanics of plasticity and fracture, Cambridge University Press, Cambridge, 1992.

[6] LEMAITRE, J., CHABOCHE, J. L., Mechanics of solid materials, Cambridge university press, Cambridge, 1994.

[7] MARŠÍK, F., Termodynamika kontinua, Academia, Praha, 1999.

[8] ŠILHAVÝ, M., The mechanics and thermodynamics of continuous media, Springer-Verlag, Berlin Heidelberg, 1997.

[9] KOZÁK, I., Kontinuummechanika, Miskolci Egyetemi Kiadó, Miskolc, 1995.

[10] BELYTSCHKO, T., LIU, W. K., MORAN, B., Nonlinear finite elements for continua and structures, John Wiley & Sons LTD, Chichester, 2000.

[11] EVANS, L. C., Partial differential equations, American Mathematical Society, Providence, Rhode Island, 1998.

[12] REKTORYS, K., Variační metody v inženýrských problémech a v problémech matematické fyziky, Academia, Praha, 1999.

[13] ÉCSI, L.: Numerical behaviour of a solid body under various mechanical loads using finite element method with new energy balance equation for fully coupled thermal-structural analysis, In proceedings of the sixth internationale congress on THERMAL STRESSES, THERMAL STRESSES 2005, TU Wien, Vienna, Austria, Vol. 2, pp. 543–546, 26–29 May 2005.

[14] ÉCSI, L., ÉLESZTŐS, P.: An attempt to simulate more precisely the behavior of a solid body using new energy conservation equation for fully coupled thermal structural analysis, In proceedings of the III. European conference on Computational mechanics: Solids, structures and coupled problems in engineering, ECCM 2006, National Laboratory of Civil Engineering, Lisbon, Portugal, 5–8. June 2006.

[15] ÉCSI, L., ÉLESZTŐS, P.: Constitutive equation with internal damping for materials under dynamic and cyclic loadings, V zborníku prednášok medzinárodnej konferencie 46th International conference in Experimental stress analysis 2008, EAN 2008, Horní Bečva,ČR, 2.-5. 6. 2008.

[16] ÉCSI, L.: Extended NOIHKH model usage for cyclic plasticity of metals, Engineering Mechanics, Vol. 13, No. 2, pp. 83–92. 2006.

[17] ÉCSI, L.: Extended NoIHKH model with damage evolution for cyclic plasticity of metals, Acta Mechanica Slovaca, Roč. 9, č. 4., pp. 95-106., 2005.

[18] LEMAITRE, J. Handbook of material behaviour models, Deformations of materials, Vol. 1, London, Academic press, 2001, 350 pp. ISBN 0-12-443342-1.

[19] TREBUŇA, F., ŠIMČÁK, F., Príručka experimentálnej mechaniky, Edícia vedeckej a odbornej literatúry, TypoPress, Košice, 2007.

[20] BUDÓ, Á., Kísérleti fizika I., Nemzeti tankönyvkiadó, Budapest, 1997.

[21] Franke, H.: Lexikon der Physik, Franckh'sche Verlagshandlung, W. Keller & Co, Stuttgart, 1959.